REPORT DOCUMENTATION PAGE

Form Approved
OMB No. 0704-0188

1. REPORT DATE *(DD-MM-YYYY)*	**2. REPORT TYPE**	**3. DATES COVERED** *(From - To)*
December 1, 2022	Final Report	July 2021- December 2022

4. TITLE AND SUBTITLE

Development of Anthropometric Specifications for the Small-Female Warrior Injury Assessment Manikin (WIAMan)

5a. CONTRACT NUMBER
DOTC-19-01-INIT0209

5b. GRANT NUMBER

5c. PROGRAM ELEMENT NUMBER
6.3

6. AUTHOR(S)

Reed, Matthew P. and Ebert, Sheila M.

5d. PROJECT NUMBER

5e. TASK NUMBER

5f. WORK UNIT NUMBER

7. PERFORMING ORGANIZATION NAME(S) AND ADDRESS(ES)

University of Michigan
Transportation Research Institute

8. PERFORMING ORGANIZATION REPORT

UMTRI-2022-10

9. SPONSORING / MONITORING AGENCY NAME(S) AND ADDRESS(ES)

US Army Ground Vehicle Systems Center

Warren, MI 48397-5000

10. SPONSOR/MONITOR'S ACRONYM(S)

11. SPONSOR/MONITOR'S REPORT NUMBER(S)
Issued Upon Submission

12. DISTRIBUTION / AVAILABILITY STATEMENT
UNCLASSIFIED -- DISTRIBUTION A. Approved for public release; distribution unlimited. OPSEC#7167

13. SUPPLEMENTARY NOTES

14. ABSTRACT

A study of female body size, shape, and posture was conducted to develop anthropometric specifications for an anthropomorphic test device (ATD) intended to represent a small-female Soldier for assessments of vehicle occupant protection in underbody blast. The small-female Warrior Injury Assessment Manikin (WIAMan) has target stature and body mass based on 5th-percentile values for female Soldiers in a recent Army study. Body landmarks and internal joint center locations were developed using data from 142 women with a wide range of body size measured in a single squad seating condition. Regression methods were used to establish target values for the ATD. Laser surface scan data from 126 women in up to four seated postures were analyzed using principal component analysis and regression to obtain a statistical model predicting body shape as a function of overall body dimensions and surface landmark locations. Small adjustments to the posture and shape were made to obtain a symmetrical posture with the thighs horizontal and legs vertical. The head surface was generated through a statistical analysis of data from a separate study that included realistic scalp contours and face landmarks. Because the hand and foot shapes were not well measured in the whole-body scan data, scaled versions of the hand and foot were added. Pelvis geometry was generated through a statistical model based on data from medical images. The final anthropometric specification included the surface geometry as a polygonal model, internal joint centers and surface landmarks, a polygonal model of the bony pelvis and sacrum, and a model of ribcage shape.

15. SUBJECT TERMS
Anthropometry, Posture, Vehicle Occupants, Statistical Shape Analysis, Safety

16. SECURITY CLASSIFICATION OF:			**17. LIMITATION OF ABSTRACT**	**18. NUMBER OF PAGES**	**19a. NAME OF RESPONSIBLE PERSON** M.P. Reed
a. REPORT UNCLASSIFIED, Dist A.	**b. ABSTRACT** UNCLASSIFIED, Dist A.	**c. THIS PAGE** UNCLASSIFIED, Dist A.		34	**19b. TELEPHONE NUMBER** *(include area code)* (734) 936-1111

Standard Form 298 (Rev. 8-98)
Prescribed by ANSI Std. Z39.18

Development of Anthropometric Specifications for the Small-Female Warrior Injury Assessment Manikin (WIAMan)

Matthew P. Reed
Sheila M. Ebert

Biosciences Group
University of Michigan Transportation Research Institute

December 2022

MICHIGAN ENGINEERING
UNIVERSITY OF MICHIGAN
TRANSPORTATION RESEARCH INSTITUTE
UNIVERSITY OF MICHIGAN

Development of Anthropometric Specifications for the Small-Female Warrior Injury Assessment Manikin (WIAMan)

Final Report

UMTRI-2022-10

by

Matthew P. Reed
Sheila M. Ebert

University of Michigan Transportation Research Institute

December 2022

ACKNOWLEDGMENTS

This work was supported by the U.S. Army Ground Vehicle Systems Center. We thank Laura Malik and Miranda St Amour, who gathered the data, as well as the many students and staff who processed data and landmarked scans.

CONTENTS

ABSTRACT

A study of female body size, shape, and posture was conducted to develop anthropometric specifications for an anthropomorphic test device (ATD) intended to represent a small-female Soldier for assessments of vehicle occupant protection in underbody blast. The small-female Warrior Injury Assessment Manikin (WIAMan) has target stature and body mass based on 5th-percentile values for female Soldiers in a recent Army study. Body landmarks and internal joint center locations were developed using data from 142 women with a wide range of body size measured in a single squad seating condition. Regression methods were used to establish target values for the ATD. Laser surface scan data from 126 women in up to four seated postures were analyzed using principal component analysis and regression to obtain a statistical model predicting body shape as a function of overall body dimensions and surface landmark locations. Small adjustments to the posture and shape were made to obtain a symmetrical posture with the thighs horizontal and legs vertical. The head surface was generated through a statistical analysis of data from a separate study that included realistic scalp contours and face landmarks. Because the hand and foot shapes were not well measured in the whole-body scan data, scaled versions of the hand and foot were added. Pelvis geometry was generated through a statistical model based on data from medical images. The final anthropometric specification included the surface geometry as a polygonal model, internal joint centers and surface landmarks, a polygonal model of the bony pelvis and sacrum, and a model of ribcage shape.

INTRODUCTION

The Warrior Injury Assessment Manikin (WIAMan) program developed a midsize-male anthropomorphic test device (ATD) for use in underbody blast testing of military vehicles and vehicle components. The anthropometric specifications for the ATD, including the body size, shape, and design posture, were based on detailed anthropometric data from the Seated Soldier Study which gathered posture and body shape data from over 300 Soldiers at three Army posts (Reed 2013). The reference body dimensions for the midsize-male WIAMan were based on 50th-percentile values for stature and body weight from a pilot study (Paquette et al. 2009) for the 2012 U.S. Army anthropometry survey, known as ANSUR II (Gordon et al. 2014). The midsize-male WIAMan was the first ATD to be based on a statistical analysis of 3D body shape data.

Recently, the data from the Seated Soldier Study were re-analyzed to create the anthropometric specifications for a large-male WIAMan (Reed 2022). The reference body dimensions were the 95th-percentile values for stature and body weight from ANSUR II.

The current report describes the development of anthropometric specifications for a small-female WIAMan, targeting the 5th-percentile female values of stature and body weight. The female data from the Seated Soldier Study were not sufficient for this purpose, because only 52 women participated in that study and sufficient 3D body shape data were only available from half that number. To address this gap, a new laboratory study of female body size and shape was conducted using methods intended to be identical to those used in the Seated Soldier study. Posture data were gathered using the same squad seating mockup, and body surface scan data were obtained using the same model laser scanner. Processing methods were also equivalent so that the data could be modeled in the same manner.

Table 1 lists the four components of the analysis. The posture target, which consists of surface landmark and internal joint center locations, was developed based on a regression analysis of landmark data from 142 female participants measured in a seat with a horizontal seat pan and vertical seat back. A statistical body shape model was created by analyzing 411 laser scans from 126 women who were each measured in four seated postures with varying levels of recline. A regression model was created to predict the body shape from overall body dimensions and a subset of the landmarks predicted for the target posture. Additional internal joint centers were interpolated to better define the spine posture. Generic hand and foot shapes were added to address limitations in the scan-based statistical model, and the posture was adjusted to the desired design posture with thighs horizontal and upper extremities in a relaxed posture.

A new 3D head shape model with an accurate scalp was available from recent work (Park et al. 2021). The female data from that study were re-analyzed to obtain an appropriate head shape, which was aligned with the whole-body shape model using surface landmarks. A larger and more-detailed set of pelvis bone shape data were also available (Brynskog et al. 2021). A regression analysis based on bispinous breadth was used to

obtain the target bone landmark configuration. These landmark data were mapped to a new 3D pelvis surface model to generate the target for the ATD.

The final body representation was compared quantitively and qualitatively with other small-female representations based on similar overall body dimensions. The Anthropometry of Motor Vehicle Occupants (AMVO) study from the 1980s developed specifications for a small-female ATD with a reference stature similar to the current work (Schneider et al. 1983). The current results were also compared with a body shape generated from a statistical model of civilian adults (Park et al. 2021a).

Table 1
Summary of Analyses, Methods, and Outcomes

Analysis	Data Source	Analysis Method	Outcome
1. Posture analysis for the WIAMan anthropometry target	Body landmark locations measured in squad condition C02 (N=142)	Regression using target stature, body weight, and ratio of sitting height to stature	Tabular data on landmark and joint locations
2. External body shape	Whole-body laser scan data in minimally clad condition, up to four seated postures per participant (N=411 scans from 126 participants)	Surface template fitting followed by principal component and regression analyses	Body surface described by a polygonal mesh with 14454 polygons corresponding to the target body dimensions and landmark locations from Analysis 1
3. Pelvis geometry	CT image analysis (N=132)	Regression analysis of landmark locations	Target landmarks and polygonal surface mesh in position
4. Head geometry	Female head surface data with complete scalp and manually identified landmarks (N=179)	Regression on combined landmark and mesh vertices	Target head shape with surface landmarks in position

METHODS

Reference Body Dimensions

The small-female WIAMan is intended to represent a "5th-percentile" Soldier. However, the target specification is better stated as "the average body size and shape for a U.S. female Soldier who is 5th percentile by stature and body weight." Because the design posture for the ATD is seated, only the target body weight can be specified directly for the design from standard anthropometric data. All other dimensions must be obtained through analysis of data from subjects who vary relative to the target values.

The reference database is ANSUR II (Gordon et al. 2012). Table 2 shows the target values for stature and body weight along with comparative values from other sources. Note that although the distribution of female stature for both military and civilian populations in the US has remained approximately the same for the past 40 years, body weight has trended upward. Although the changes in the lower quantiles of the distribution have been smaller than in the upper quantiles, the target body weight of 51.3 kg (113.1 lb) is about 10% larger than the civilian value from the 1980s used in the specification of the Hybrid-III "5th-percentile" female. The stature value from the US Army 1988 ANSUR survey is similar to the current value, and the current body weight value is only 1.6 kg (3.5 lb) higher than the corresponding value from 1988. For reference, the current 95th-percentile values for U.S. civilian women ages 20-29 (Fryar et al. 2021) are 25 mm smaller for stature but similar for body weight.

Table 2
Male Reference Dimensions Compared with Previous Studies

Dimension (95th-percentile values)	WIAMan Target*	ANSUR 88**	Small-Female AMVO Target (Schneider et al. 1983)	Hybrid-III (95th-percentile)†	Civilians Ages 20-29††
Stature (mm)	1525	1529	1511	1513	1498
Body Mass (kg)	51.3	49.7	47.3	46.7	49.8
BMI*** (kg/m^2)	22.1	21.5	20.7	20.4	22.2
Stature (in)	60.0	60.2	59.5	59.6	60.0
Body Mass (lb)	113.1	109.6	104.3	103.0	109.8

* ANSUR II
** 5th-percentile female values
*** BMI for the 5th-percentile values of stature and weight, rather than 5th-percentile BMI.
† Reference values from Mertz et al. 2001
†† Values for civilian women ages 20-29 years from Fryar et al. 2021.

Laboratory Data Collection

Participants

Data were gathered from a convenience sample of 142 female adults ages 18 to 31 years (mean age 24 years). By design, the sample was biased toward smaller women, with relatively few women with high stature or body weight. Figure 1 shows stature and body weight for the sample, along with the target values for reference. Sampling for low body weight was more successful than sampling for low stature, with 13% of the participants having stature within 25 mm of the ATD reference value and 38% of the participant having body weight within 5 kg of the target. In addition to stature and body weight, 33 standard anthropometric measurements were obtained from each participant. Methods were based on ANSUR II.

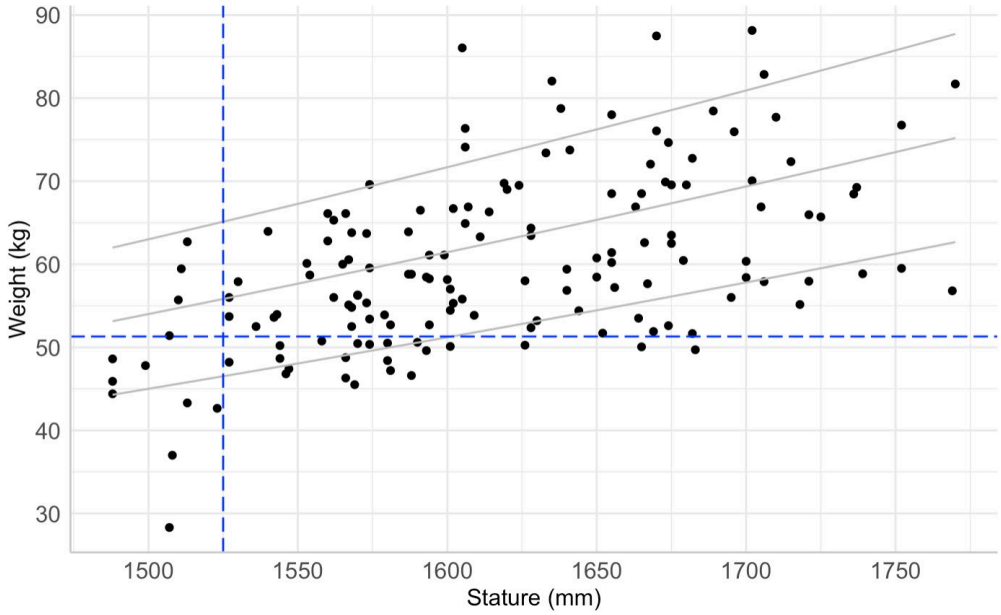

Figure 1. Participant stature and body weight. Curves illustrate BMI 20, 24, and 28 kg/m^2. Dashed lines show the ATD reference dimensions of 1525 mm and 51.3 kg.

Posture Measurement

Participants were instructed to sit comfortably in the seat shown in Figure 2. Lower and upper extremity postures were required to be approximately symmetrical, with the legs vertical so that the ankles were below the knees. The hands rested on the top of the thighs. A FARO Arm coordinate digitizer was used to record body landmark locations defining the seated posture. The posture data for the current analysis were extracted from Condition C02, in which the padded seat back was nominally vertical, the padded seat cushion was nominally horizontal, and the seat height above the floor (measured from

SAE J826 H-point) was 350 mm (for more details, see Reed and Ebert 2013). This seat height, which is 100 mm lower than the seat height used for the large male analysis, was chosen to allow even the smallest participants to sit comfortably with their legs vertical and shoes resting comfortably on the floor.

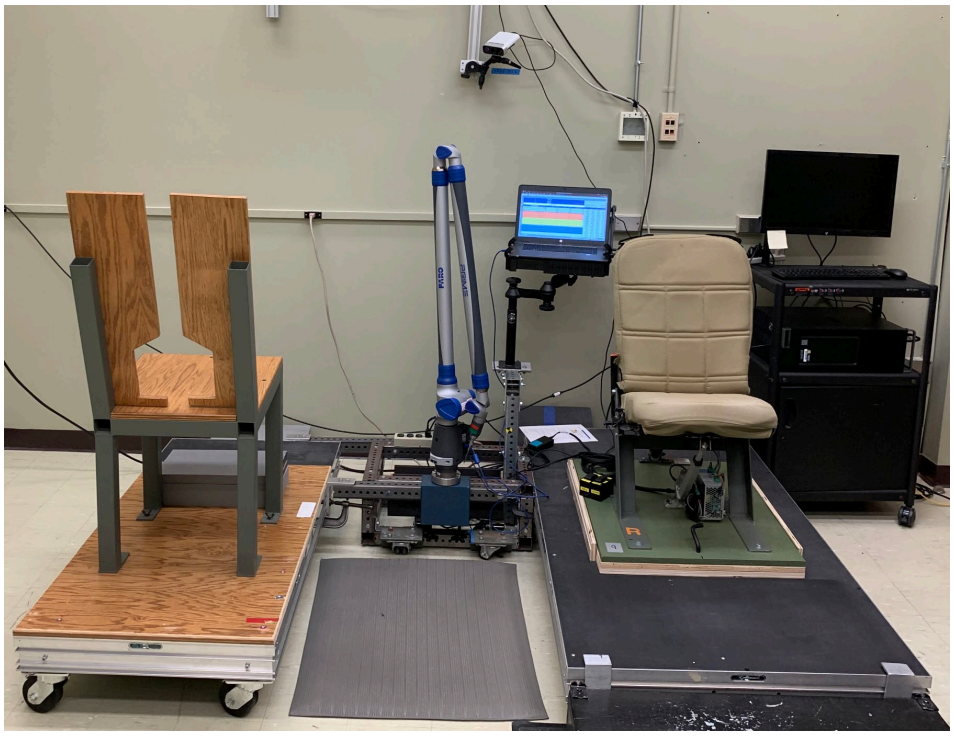

Figure 2 Squad seat mockup (right) and hardseat (left).

Hardseat Data and Analysis

Additional data obtained in a laboratory hardseat, shown in Figure 2, were used to augment the data from the padded test seat. The hardseat provided access to posterior landmarks, enabling a more accurate characterization of each soldier's pelvis and spine geometry. These data were used to estimate pelvis and spine joint center locations relative to surface landmarks. The relationships between the anterior landmarks accessible in the squad seat and the joints were used to estimate joint center locations in the squad seating conditions. For more details on these calculation procedures, see Reed and Ebert (2013).

Body Landmark and Joint Analysis Methodology

The goal of the landmark analysis was to obtain a consistent set of landmarks and joint center location estimates for individuals who match the reference body dimensions. In most previous analyses of this type (e.g., AMVO), data from individuals judged to be "close" to the reference size were averaged. The current analysis uses a more rigorous regression procedure that allows data from individuals with a wide range of body size to

be used. Each landmark or joint coordinate is regressed on stature and body mass index, and the reference values described above are then input to the resulting equations. To facilitate the interpretation of the analysis, the regressions were performed on principal components (PCs) of the covariance matrix of the landmark coordinates, but all PCs were retained, so the results are equivalent to regression on the individual coordinates. No tests of statistical significance were performed, because excluding non-significant terms would result in inconsistencies across landmarks in trends with body size. For example, BMI was included as a predictor in the regression models for all PCs, even though it was only statistically significant for a few of the PCs.

A rationalization process was applied to obtain symmetrical landmarks. The Y (lateral) coordinates of landmarks on the midline of the body were assigned a value of zero, eliminating small asymmetries, typically less than a millimeter, that remained after the statistical modeling process. Bilateral pairs of landmarks (for example, left and right acromion) were assigned X and Z values equal to the means of the respective points, and the Y values were set to ± 50% of the initial Y-axis difference between the points.

The output of this analysis and rationalization process was a list of landmark and joint locations that represent the initial target for the ATD. As noted below, some additional posture adjustments were conducted to obtain the desired reference posture.

External Body Shape

Laser Scan Data Processing

Laser scan data were obtained using a VITUS XXL laser scanner. The scanner records about 500k surface data points during a scanning interval of 12 seconds. A total of 411 scans from 126 participants were used in the analysis of body shape, with up to four scan postures per participant. Figure 3 shows the postures. Due to the study design, this is a different subset of the participants than was used for the posture analysis. Note that the analysis techniques are robust to differences in the samples. Surface body landmark locations were manually extracted from the scan data, as described in Reed and Ebert (2013).

The current analysis used a template mesh that differed from the one used in Reed (2013) for the midsize male. The new template is symmetrical and based on quadrilaterals rather than triangles. The template was initially morphed to match the data at a subset of the landmarks, followed by a "fine-fitting" step that moved the template landmarks into the surface defined by the target scan data. A second round of template fitting was conducted using a "bootstrap" prediction model. That is, a statistical body shape model was generated using the data from the first round of fitting that predicted body shape from the landmarks. This was used in place of the landmark-based morphing step for the second round of fitting.

To generate the final statistical body shape model, a principal component analysis (PCA) was conducted on the vertex coordinates. For the subsequent regression analysis to

predict body shape, 60 PCs representing over 99 percent of the variance in the coordinate data were retained.

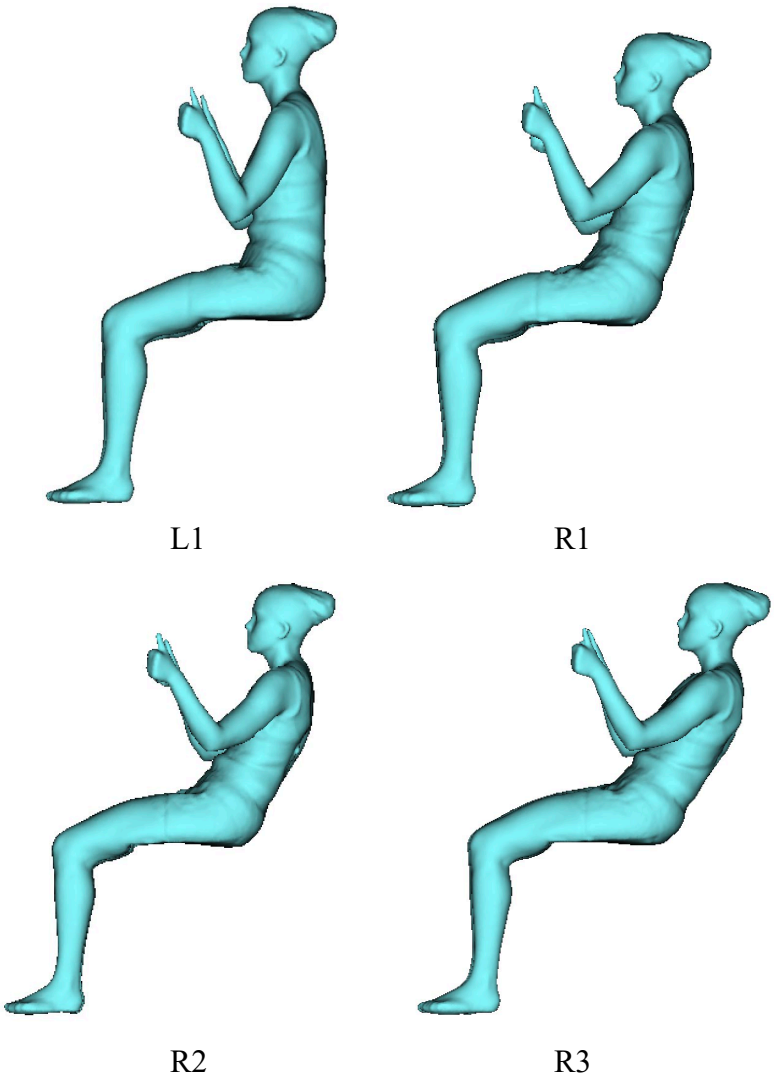

Figure 3. The four scan postures used for the current analysis. Postures R1, R2, and R3 were supported by a small, padded backrest (see Reed and Ebert 2013 for details).

The body shape analysis proceeded somewhat differently from the landmark analysis. One approach would be to conduct a regression analysis to predict PC scores from the reference body dimensions in the same manner as with the landmark data. However, because the scan and landmark data were drawn from different conditions, some discrepancies would inevitably emerge. Consequently, a set of landmark joint locations were used along with the body dimensions as input to the body shape predictions. Table 3lists the landmarks and joints. All landmarks and joints were included in the PCA of the body shape data, enabling verification that the landmark and joint targets were met (all discrepancies < 0.1 mm).

Table 3
Surface Landmarks and Joints Used Along with Stature and BMI to Predict the Body Surface Shape

Glabella_Ct_L	SpineT04_Ct_M
Tragion_Rt_L	SpineT12_Ct_M
Tragion_Lt_L	SpineL03_Ct_M
Suprasternale_Ct_L	L5S1Joint
Substernale_Ct_L	HipJntRt
SpineC07_Ct_M	HipJntLt

Posture Adjustment

The desired design posture for the WIAMan included a horizontal thigh segment, a vertical leg, and a relaxed upper-extremity posture. Because the posture and body shape data were obtained with a different seat height and arm posture, the posture of the predicted body shape was adjusted using linear blend skinning. Under this common approach to pose modification, each vertex in the model is assigned a weight for each adjacent body segment. For example, joints near the elbow have weights for the forearm and arm segments. When the model is articulated, each vertex is moved according to the weights for these segments. The result is a smooth blending at the joints.

Spine Joint Interpolation

The surface landmark data were used directly to estimate spine joints at the atlanto-occipital junction, C7/T1, T12/L1, and L5/S1. To provide additional guidance for ATD design, the intervening joint centers, defined as the estimated geometric centers of the intervertebral disks, were estimated from the surface contour by interpolating between the previously calculated joint centers. The motion segment heights (e.g., L4/L5 to L5/S1) were determined as fractions of the lumbar, thoracic, and cervical chord lengths using data from Black et al. (1991).

Head Geometry

The whole-body surface model uses data from a laser scanner that does not provide a high level of detail on the face and head. Moreover, the data are affected by hair artifacts, such that the scalp shape is not accurately captured. For the midsize male WIAMan, an analysis of head and face landmark and measurement data was used to morph a reference head model (Reed and Corner 2013). However, a new model based on detailed head scans from 179 women was available for the small-female analysis (Park et al. 2021b). The model is based on data obtained using a manual measurement method that enables accurate scalp measurement. A statistical model created from these data was generated using the same template mesh used for the whole-body modeling. A total of 58 manually identified landmarks were included in the statistical model, which predicted head shape from head length, head breadth, and tragion to top of head. These manually measured dimensions are available in the ANSUR II dataset. A regression analysis with ANSUR II data using stature and BMI as predictors gave target values of length = 184 mm, breadth = 146 mm, and tragion to top of head = 123 mm (Table 4). These values were used to

generate a head model that was then slightly scaled (less than 3 mm per axis) to match the target values. Table 4 demonstrates that because the head dimensions are not highly correlated with stature or body weight the percentage difference in head dimensions between the midsize male and small female is smaller than the difference in stature and body weight.

Table 4
Comparison of Small-Female, Midsize-Male, and Large-Male Target Head Dimensions†

	Stature (mm)	Weight (kg)	BMI (kg/m^2)	Head Length (mm)	Head Breadth (mm)	Tragion to Top of Head (mm)
Small Female	1525	51.3	22.1	184	146	123
Midsize Male	1755	84.2	27.3	199	154	131
Large Male	1870	110.7	31.7	206	157	134
Ratio LM/MM*	6.6%	31.5%	16.1%	3.5%	1.9%	2.3%
Ratio SF/MM**	-13.1%	-39.1%	-19.0%	-7.5%	-5.2%	-6.1%

* (large male – midsize male)/midsize male * 100%
** (small female – midsize male)/midsize male * 100%
† Note that ATD head may have different dimensions due to design, manufacturing, and performance requirements.

Pelvis Geometry

The external body landmark measurements obtained using the FARO Arm in the laboratory seats provide good information on the position and orientation of the pelvis, but the data are insufficient to specify the overall size and shape of the pelvis. To provide detailed guidance for ATD design, an analysis of medical imaging data was conducted.

The current analysis used the same dataset that was used for the large male. Brynskog et al. (2021) extracted 286 landmarks from each of 57 male and 74 female pelves extracted from computed tomography (CT) studies of adults with a wide range of body size. For the current analysis, a regression model expressed the landmark locations as a function of bispinous breadth (distance between the anterior-superior iliac spine landmarks). The regression model included an interaction term for sex. The target bispinous breadth was obtained by regression in the ANSUR dataset (Gordon et al. 1989), which includes manually measured bispinous breadth (bispinous breadth is not available in ANSUR II). The target value for 1525 mm stature was given by 66.9 + 0.0938*stature = 210 mm. Note that because pelvis size is only weakly correlated with overall body size, the target value is only 22 mm smaller than the target value for the midsize male. However, the shape of the pelvis is substantially different due to the main effect of sex in the regression model.

The predicted landmarks were rationalized by making the left and right sides symmetrical and assigning landmarks on the mid-sagittal plane a lateral coordinate value of zero. The resulting landmark configuration was then translated and rotated to align with joint locations estimated from the surface body landmarks. A generic midsize-male pelvis surface model developed in previous UMTRI research was morphed to the current target

using radial-basis-function techniques (Bennink et al. 2007) to match the target landmark configuration, providing geometric guidance for the overall bony pelvis and sacrum.

Hands and Feet

During the development of the midsize-male WIAMan ATD, a substantial amount of design effort was needed to adapt the target foot model from Reed and Corner (2013) to the ATD, which requires a contoured sole to fit appropriately in a boot. The hand, which has minimal importance for the performance of this ATD, was created by scaling existing geometry.

Consequently, for the small-female ATD, scale factors were generated that could be used to adjust the midsize-male WIAMan hand and foot geometry to the appropriate targets. The scale factors were generated using ANSUR II data by the following process:

1. Select reference dimensions: foot length, foot breadth, ankle height, hand length, and hand breadth.
2. Generate linear regression equations predicting the dimensions from stature and BMI.
3. Using the regression equations, compute expected values for the midsize male and small female.
4. Calculate the scaling ratios as a percentage: (small female value – midsize mal)/(midsize male value) * 100%

For the foot, the scale factors were -15%, -19%, and -19% for the length, width, and height, respectively. For the hand, -15% for both length and width. Note that these are similar to the stature ratio (1525-1755)/1755 = -13%.

RESULTS

Posture Analysis for the Small-Female WIAMan Anthropometry Target

Landmarks and Joints

Tables 5A-5C list landmark and joint locations calculated using the regression methods described above. The X axis is positive rearward, the Y axis is positive to the right, and the Z axis is positive upward. The origin is the midpoint between the hip joint centers. The thigh segments (hip to knee) are in the horizontal plane through the hips, and the ankles are in the vertical sagittal plane through the knee joints.

Table 5A
Extremity Joint Centers (mm)

Name*	X (fore-aft)	Y (lateral)	Z (vertical
ShoulderJnt_L	36.8	-172.2	408.7
ElbowJnt_L	-22.9	-219	191.6
WristJnt_L	-246.9	-212.1	184.5
KneeJnt_L	-385	-129.4	0
AnkleJnt_L	-385	-129.4	-345.4
HipJnt_R	0	86.2	0
HipJnt_L	0	-86.2	0
ShoulderJnt_R	36.8	172.2	408.7
ElbowJnt_R	-22.9	219	191.6
WristJnt_R	-246.9	212.1	184.5
KneeJnt_R	-385	129.4	0
AnkleJnt_R	-385	129.4	-345.4

Table 5B
Surface Landmarks (mm)

Name*	X (fore-aft)	Y (lateral)	Z (vertical
Suprasternale	-0.6	0	448.9
Substernale	-65.3	0	242.3
C7Surface	36.5	0	590.4
T4Surface	107.9	0	509.9
T8Surface	138	0	441.8
T12Surface	156.7	0	262.9
L1Surface	148.8	0	214.7
L2Surface	142.9	0	189.6
L3Surface	138	0	160.9
L4Surface	133.8	0	133.8
L5Surface	131.5	0	103.3
Tragion_L	21.2	-76	609.3
Acromion_L	30.5	-167.2	467.6
HumeralEpiCon_Lat_L	-31.7	-244.9	203.6
Wrist_Lat_L	-236.9	-231	188.7
FemoralEpiCon_Lat_L	-389.3	-163.3	2.8
Suprapatella_L	-413.7	-128.7	46.2
Infrapatella_L	-433.6	-128.7	-10.5
Malleolus_Lat_L	-389.3	-163.3	2.8
Tragion_R	21.2	76	609.3
Acromion_Ant_R	30.5	167.2	467.6
HumeralEpiCon_Lat_R	-31.7	244.9	203.6
Wrist_Lat_R	-236.9	231	188.7
FemoralEpiCon_Lat_R	-389.3	163.3	2.8
Suprapatella_R	-413.7	128.7	46.2
Infrapatella_R	-433.6	128.7	-10.5
Malleolus_Lat_R	-406.3	148.9	-339.6
ASIS_L	-33.8	-111.6	92.1
ASIS_R	-33.8	111.6	92.1

* Suffixes L and R indicate the left and right side of the body, respectively. Origin is midpoint between the hip joint centers.

Table 5C
Spine Joint Centers (mm)

Name*	X (fore-aft)	Y (lateral)	Z (vertical
L5S1Joint	64.7	0	86.8
L4L5Joint	70.1	0	118.5
L3L4Joint	76.6	0	149.7
L2L3Joint	84.2	0	180.2
L1L2Joint	92.5	0	209.7
T12L1Joint	100.1	0	238.5
T11T12Joint	105.4	0	264.7
T10T11Joint	107.1	0	289.5
T9T10Joint	105.8	0	312.9
T8T9Joint	102.3	0	334.8
T7T8Joint	97.4	0	355.5
T6T7Joint	91.8	0	375.7
T5T6Joint	85.6	0	395.4
T4T5Joint	79.2	0	414.3
T3T4Joint	72.6	0	432.6
T2T3Joint	66	0	450.2
T1T2Joint	59.5	0	467
C7T1Joint	53.3	0	482.9
C6C7Joint	51.3	0	483
C5C6Joint	45.8	0	498.6
C4C5Joint	41.4	0	513.5
C3C4Joint	37.8	0	527.8
C2C3Joint	34.8	0	542.5
C1C2Joint	33.3	0	557.7
HeadNeckJnt	36.5	0	590.4

* Spine joint centers are estimated at the geometric center of the associated disk. HeadNeckJnt (atlanto-occipital joint) is estimated at the geometric center of the arc of the occipital condyles.

Segment Length Comparison

One consideration in evaluating the current results is a comparison of the segment lengths with other "small female" representations (nominally "5th-percentile female"). Table 6 lists comparative data from AMVO and the Hybrid-III ATD family. Note that the AMVO values differ somewhat from the original publication in Schneider et al. (1983). To provide better comparability with the current work, the joint locations were calculated using the methods in Reed et al. (1999) from the AMVO shell surface landmark locations.

The largest differences are seen in the thorax and abdomen (lumbar) segments. The sum of the two segment lengths differs by only 3 mm, but the thorax in the current analysis is 43 mm shorter. This difference results from a substantial change in the way the thorax length was estimated. Specifically, the current value is based on a statistical model of the thorax developed from analysis of CT data (Wang et al. 2016). We regard this estimate as being more accurate than the estimates developed during the AMVO program in the 1980s, which used scaling relationships developed using a small set of lateral radiographs of men taken in an earlier study. The current analysis based on CT data indicates that the thorax segment length is on average approximately 61% of the total of the thorax and lumbar segment lengths for both men and women regardless of overall body size.

Table 6
Segment Length Comparison (mm)

Segment	Definition	Current	AMVO†
Neck	AO-C7/T1	111	101
Thorax	C7/T1-T12/L1	242	285
Abdomen	T12/L1-L5/S1	161	115
Pelvis	L5/S1-mean hip joint center	108	92
Thigh	Hip-Knee	412	398
Leg	Knee-Ankle	346	342
Arm	Glenohumeral-Elbow	231	257
Forearm	Elbow-Wrist	224	228

† Joint locations in AMVO were calculated from the small-female shell landmark locations reported in Schneider et al. (1983) using methods from Reed et al. (1999) for improved consistency with the current methods.

External Body Shape

Figure 4 shows the initial body shape and landmarks generated from the statistical shape model using the target landmarks and body dimensions. The upper and lower extremity postures reflect the scan postures, which included a slight downward angle of the thighs and the upper extremities abducted and flexed at the shoulder and elbow. At this stage of

the analysis, the surface and landmarks are not yet symmetrical, and the head, hands, and feet are not yet finalized.

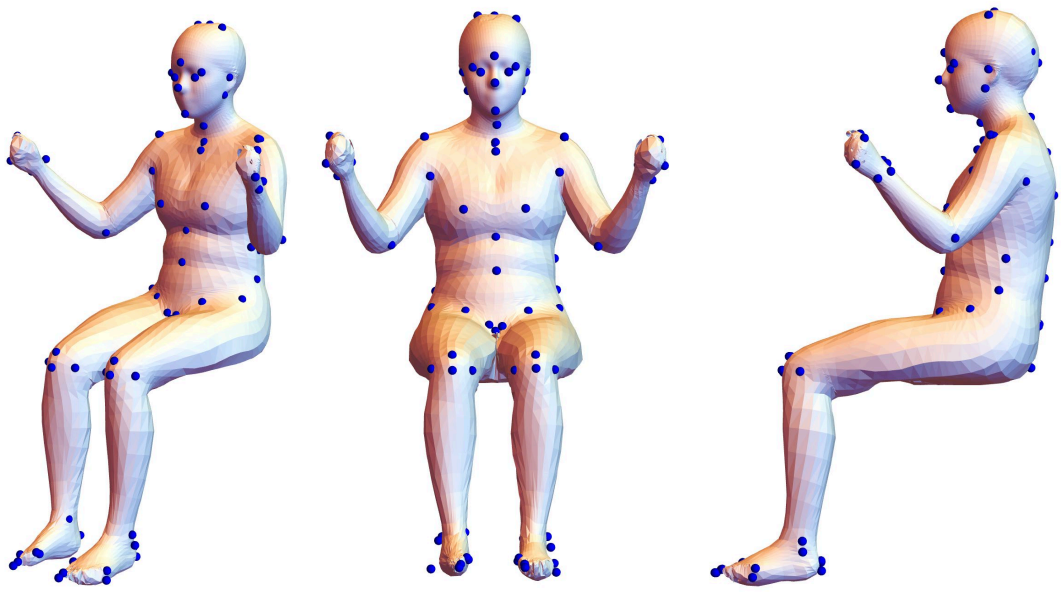

Figure 5. Body shape output from the regression model prior to posture and shape adjustments.

Figure 6 shows the target head geometry. The landmark locations in the whole-body coordinate system are listed in Tables 7A-7C. Because the head model was developed on the same mesh used for whole-body fitting, the head could be easily aligned and merged using the common landmarks.

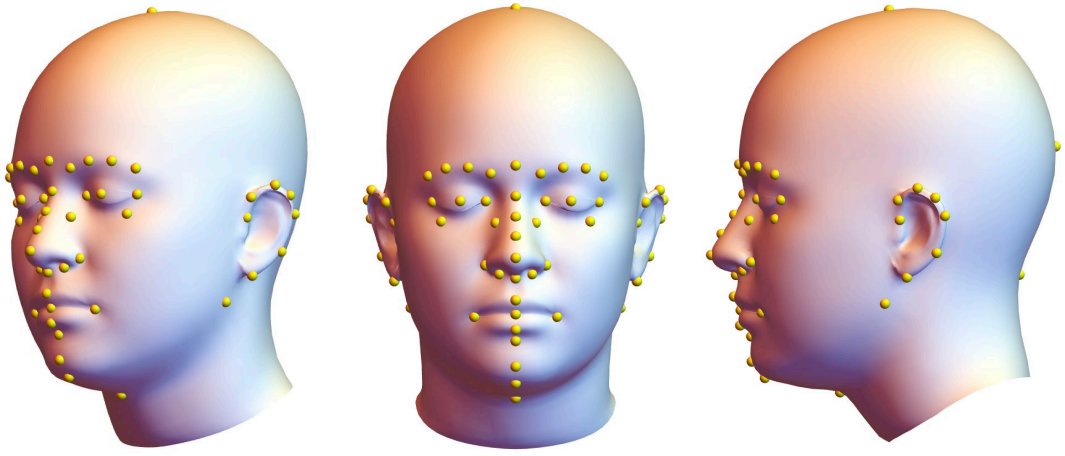

Figure 6. Head shape with landmarks.

Table 7A
Head Landmarks Group A (mm)

X	Y	Z	Landmark Name
21.2	-68.7	609.3	EarTragion_R
20	-73.6	620.7	Ear_Preaurale_R
31.3	-81.8	627.8	Ear_Superaurale_R
41.5	-83.8	622.3	Ear_Half_Super_Post_R
47.2	-82.1	611.8	Ear_Postaurale_R
42.7	-75.8	590.3	Ear_Half_Post_Sub_R
25.6	-68.9	575.9	Ear_Subaurale_R
21.2	68.7	609.3	EarTragion_L
20	73.6	620.7	Ear_Preaurale_L
31.3	81.8	627.8	Ear_Superaurale_L
41.5	83.8	622.3	Ear_Half_Super_Post_L
47.2	82.1	611.8	Ear_Postaurale_L
42.7	75.8	590.3	Ear_Half_Post_Sub_L
25.6	68.9	575.9	Ear_Subaurale_L
-60.9	-31.5	620.9	EyeCen_R
-60.9	31.5	620.9	EyeCen_L
-57.2	-17	620.9	Eye_CorMed_R
-57.2	17	620.9	Eye_CorMed_L
-47.4	-47.1	620.5	Eye_CorLat_R
-47.4	47.1	620.5	Eye_CorLat_L
-50.7	-42.2	609.2	Eye_Infraorbiatale_R
-50.7	42.2	609.2	Eye_Infraorbiatale_L
-55.2	-12.5	607.2	Eye_CtInfraorbiatale_R
-55.2	12.5	607.2	Eye_CtInfraorbiatale_L

Table 7B
Head Landmarks Group B (mm)

X	Y	Z	Landmark Name
-68.2	-14.2	636.5	EyebrowMed_R
-66.5	-27	639.9	EyebrowMedQuart_R
-60.7	-39.7	639.5	EyebrowLatQuart_R
-51.1	-49.6	635.1	EyebrowLat_R
-68.2	14.2	636.5	EyebrowMed_L
-66.5	27	639.9	EyebrowMedQuart_L
-60.7	39.7	639.5	EyebrowLatQuart_L
-51.1	49.6	635.1	EyebrowLat_L
-70.9	0	641.1	Head_Glabella
-72.4	0	576.8	Nose_Subnasale
-68.3	0	623.6	Nose_Sellion
-73.7	0	611.7	Nose_Rhinion
-80.9	0	600.5	Nose_Supratip
-86.9	0	588.3	Nose_Pronasale
-65.1	-11.3	608.3	Nose_Width_R
-65.1	11.3	608.3	Nose_Width_L
-64.2	-17.2	584.2	Nose_AlarCurve_R
-64.2	17.2	584.2	Nose_AlarCurve_L
-68.5	-9.2	579.2	Nose_Subalare_R
-68.5	9.2	579.2	Nose_Subalare_L

Table 7C
Head Landmarks Group C (mm)

X	Y	Z	Landmark Name
-57.7	-23.4	555	Lips_Chelion_R
-57.7	23.4	555	Lips_Chelion_L
-73.5	0	564.3	Lips_LabialeSup
-69.6	0	556.3	Lips_Stomion
-69.8	0	547.5	Lips_LabialeInf
-63.3	0	541.1	Lips_Sublabiale
-55.2	0	517.1	Chin_Gnathion
-62.9	0	526.5	Chin_Pogonion
-11.5	0	509	Chin_Cervical
13.1	-59.5	560.6	Gonion_R
13.1	59.5	560.6	Gonion_L
15.6	0	731.1	HeadTop
112.8	0	652.5	HeadBack
92.3	0	578	Head_Occiput

Pelvis Geometry

Tables 8A and 8B list selected pelvis landmark locations in the WIAMan design position. Figure 7 shows the pelvis geometry at the design orientation from several angles.

Table 8A
Pelvis Landmarks Group A (mm)

X*	Y	Z	Landmark
-12.8	-104.5	82.2	1_ASIS_L
-12.8	104.5	82.2	2_ASIS_R
-11.9	-90.6	43.6	4_AIIS_L
-11.9	90.6	43.6	5_AIIS_L
-5.1	-96.1	60.2	6_AS_mid_L
-5.1	96.1	60.2	7_AS_mid_R
123.3	-47.0	38.6	8_PSIS_L
123.3	47.0	38.6	9_PSIS_R
-45.7	-3.0	2.4	16_PS_Sup_L
-45.7	3.0	2.4	20_PS_Sup_R
57.6	-0.6	68.8	24_S1_Ant
85.6	-0.8	77.6	25_S1_Post
71.8	-24.2	75.7	26_S1_Left
71.8	24.2	75.7	27_S1_R
77.3	1.0	-40.1	32_Coccyx
-2.7	-50.4	-67.9	87_IT_L
-2.7	50.4	-67.9	93_IT_R
0	-86.2	0	HipJntLt
0	86.2	0	HipJntRt

* Origin is at midpoint between hip joint centers. X is fore-aft, Y is lateral, Z is vertical

Table 8B
Pelvis Landmarks Group B (mm)

X*	Y	Z	Landmark
6.1	-119.2	93.0	33_LatIliacCrest1_L
31.1	-127.7	95.2	34_LatIliacCrest2_L
57.2	-124.0	97.2	35_LatIliacCrest3_L
79.3	-108.6	101.8	36_LatIliacCrest4_L
97.9	-88.8	98.7	37_LatIliacCrest5_L
111.9	-69.5	85.3	38_LatIliacCrest6_L
121.6	-59.3	62.0	39_LatIliacCrest7_L
6.1	119.2	93.0	47_LatIliacCrest1_L
31.1	127.7	95.2	48_LatIliacCrest2_R
57.2	124.0	97.2	49_LatIliacCrest3_R
79.3	108.6	101.8	50_LatIliacCrest4_R
97.9	88.8	98.7	51_LatIliacCrest5_R
111.9	69.5	85.3	52_LatIliacCrest6_R
121.6	59.3	62.0	53_LatIliacCrest7_R
-0.4	-72.9	-20.0	67_Acet1_L
22.6	-95.6	-5.1	69_Acet2_L
0.3	-95.5	23.2	71_Acet3_L
-16.3	-68.5	3.7	73_Acet4_L
-0.4	72.9	-20.0	75_Acet1_R
22.6	95.6	-5.1	77_Acet2_R
0.3	95.5	23.2	79_Acet3_R
-16.3	68.5	3.7	81_Acet4_R

* Origin is at midpoint between hip joint centers. X is fore-aft, Y is lateral, Z is vertical.

Figure 7. Pelvis geometry and landmarks at design orientation.

Ribcage

A ribcage was generated using an updated version of a statistical model of the thoracic skeleton developed in prior work (Wang et al. 2016). The ribcage was positioned within the body shape using the associated spine landmarks (C7/T1 and T12/L1).

Complete Prediction

Figure 8 shows the complete prediction with skeletal linkage, pelvis, and ribcage. For comparison, Figure 9 shows the body shape overlaid with the AMVO small female shell. The overall size is similar, but the current model has greater chest and abdomen depth, reflecting the higher BMI. Figure 10 shows an overlay with a body shape created using a statistical model of women in a driving posture published online at HumanShape.org (Park et al. 2021a). The inputs were the WIAMan target stature and BMI. The body size matches closely, with the WIAMan slightly wider in the hips and deeper in the torso.

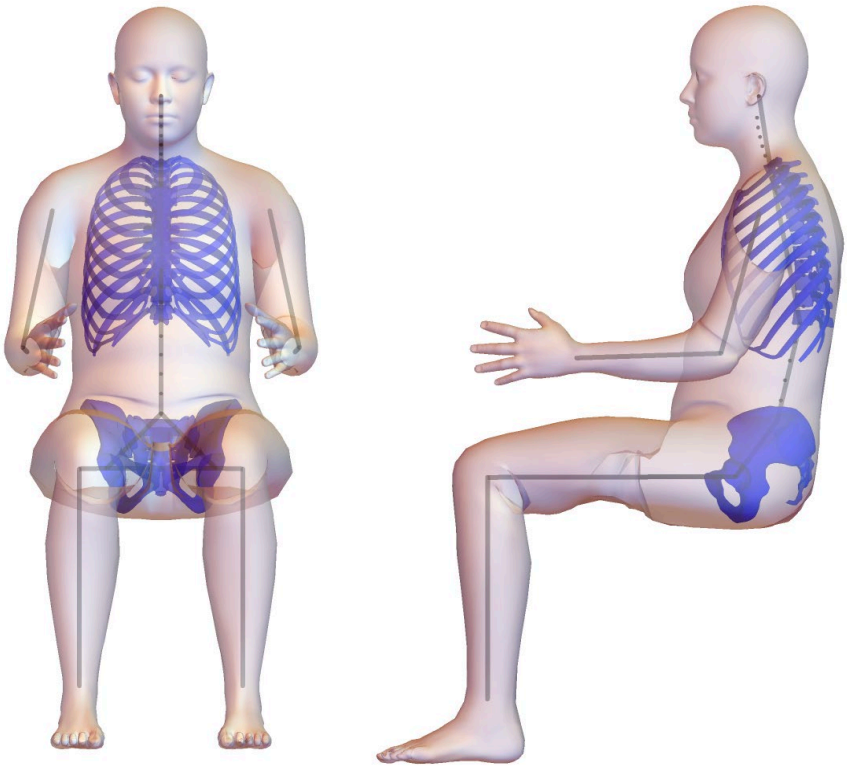

Figure 8. Final body shape after posture adjustment with landmarks, joints, and integrated head, hands, and feet. See Tables 5A-5C for quantitative information on landmark and joint locations.

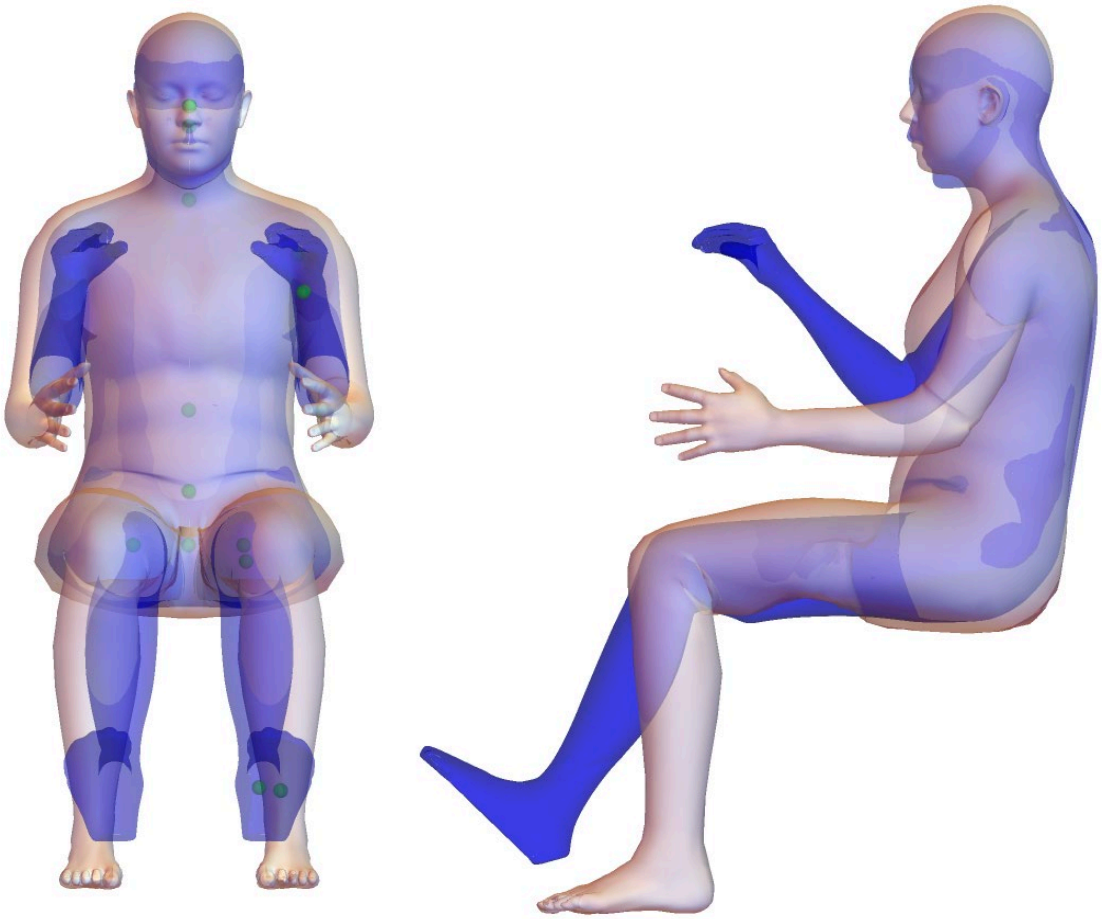

Figure 9. Comparison of the small-female WIAMan external body shape with the small-female AMVO shell (blue). The AMVO shell was aligned to the small-female WIAMan shell at the hip joints and rotated around the Y axis to align at the cervicale (C7 surface) landmark. The AMVO shell represents a typical driving posture with a seat back angle of about 23 degrees.

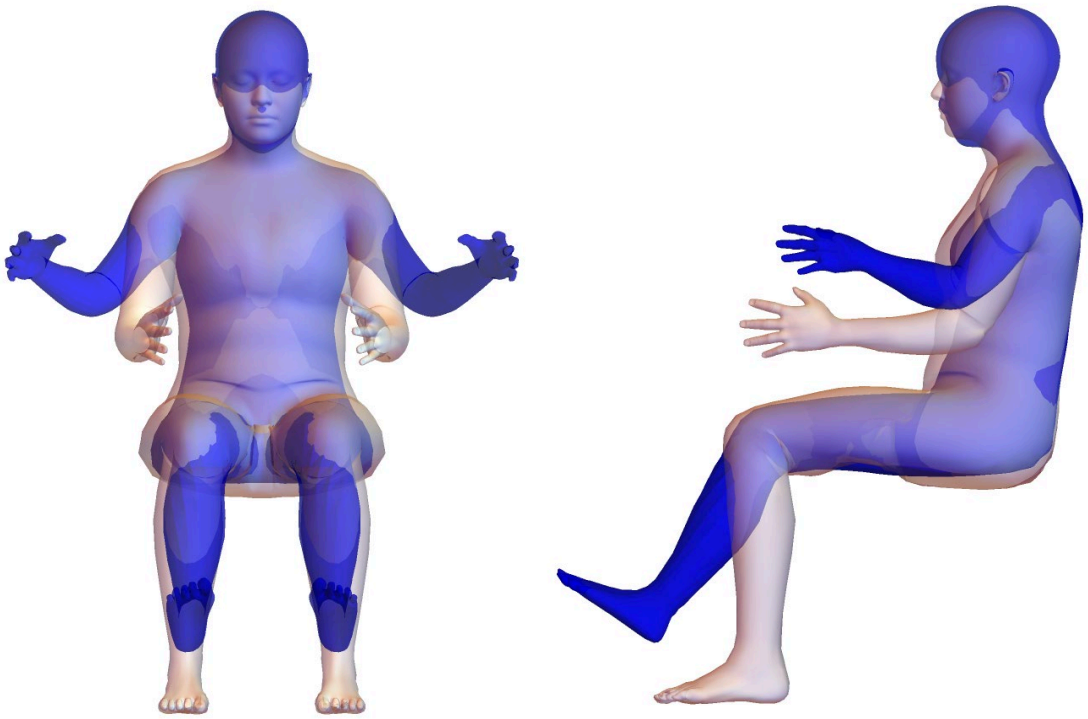

Figure 10. Comparison of the small-female WIAMan external body shape with a HumanShape small-female shell (blue) generated using a statistical body shape model for civilians (Park et al. 2021a, HumanShape.org). The HumanShape shell was aligned to the small-female WIAMan shell at the hip joints and rotated around the Y axis to approximately align the upper thorax. The HumanShape shell represents a typical driving posture with the arms abducted.

DISCUSSION

The small-female anthropometric specification presented here is the first available to be based on young adult data and to be developed for an upright posture. The three WIAMan anthropometric specifications are the first ATD shapes to be developed using a statistical analysis of whole-body shape. As with the recently developed large male (Reed 2022), the small female has head, pelvis, and ribcage geometry based on statistical models that were not available during the development of the midsize male.

As with all empirical studies, the work is limited by the composition of the dataset used for each of the analysis components. Because the target stature and weight are both in the extreme lower tail for the population, few female participants could be recruited that closely matched both criteria. However, the regression methods used for this analysis enable data from women with a wide range of body size to be incorporated into the calculations. Among the advantages of this approach is that additional body sizes, such as midsize female, can be generated with minimal additional effort.

Unlike the male ATD specifications, the current work is based on data from civilians. Military women who are close to the target specifications may have a somewhat different body shape, on average. However, the discrepancies are likely to be small, because the current sample is based on young women and because people with low BMI exhibit less body shape variability.

The data from this study were gathered using methods that were essentially identical to those used for squad posture and body shape measurement in the Seated Soldier Study. Consequently, these datasets can be merged for future analyses.

An ATD built from these specifications would be expected to differ in some ways. Notably, the ATD buttock and thigh shape would be adjusted to best reflect the fabrication and performance requirements, including removing the seat-related anomalies in the posterior thigh area. Differences would also be expected in the joint areas to reflect the range of motion requirements for the ATD. Simplifications of details in the face and other areas could also be expected.

REFERENCES

Bennink, H.E., Korbeeck, J.M., Janssen, B.J., and Romenij, B.M. (2006). Warping a neuro-anatomy atlas on 3D MRI data with radial basis functions. *Proceedings of the 2006 International Conference on Biomedical Engineering*. pp. 214-218.

Black, D.M., Cummings, S.R., Stone, K., Hudes, Palermo, L., and Steiger, P. (1991). A new approach to defining normal vertebral dimensions. Journal of Bone and Mineral Research, 6(8):883-892.

Brynskog, E., Iraeus, J., Reed, M.P., and Davidsson, J. (2021). Predicting pelvis geometry using a morphometric model with overall anthropometric variables. *Journal of Biomechanics*, 126. 10.1016/j.jbiomech.2021.110633

Fryar, C.D., Carroll, M.D., Gu, Q/, Afful. J., and Ogden, C.L. (2021). Anthropometric reference data for children and adults: United States, 2015–2018. National Center for Health Statistics. Vital Health Stat 3(46).

Gordon CC, Churchill T, Clauser CE, Bradtmiller B, McConville JT, Tebbetts I, and Walker RA (1989) *1988 Anthropometric Survey of U.S. Army Personnel: Methods and Summary Statistics*. NATICK/TR-89/044. U.S. Army Natick Soldier Research, Development, and Engineering Center, Natick, MA.

Gordon, C. C., Blackwell, C. L., Bradtmiller, B., Parham, J. L., Barrientos, P., Paquette, S. P., and Mucher, M. (2014). 2012 Anthropometric Survey of Marine Corps Personnel: Methods and Summary Statistics. (NATICK/TR-15/007). Army Natick Soldier Research Development and Engineering Center, Natick, MA.

Mertz, H.J, Jarrett, K., Moss, S., Salloum, M., and Zhao, Y. (2001). The Hybrid III 10-year-old dummy. *Stapp Car Crash Journal,* 45:319-328.

Paquette, SP, Gordon CC, and Bradtmiller B (2009) *ANSUR II Pilot Study: Methods and Summary Statistics*. NATICK/TR-09/014. U.S. Army Natick Soldier Research, Development, and Engineering Center, Natick, MA.

Park, B. K. D., Jones, M. L., Ebert, S., and Reed, M. P. (2021a). A Parametric Modeling of Adult Body Shape in a Supported Seated Posture Including Effects of Age. *Ergonomics*. 10.1080/00140139.2021.1992020.

Park, B-K., Corner, B.D., Hudson, J.A., Whitestone, J., Mullenger, C.R., and Reed, M.P. (2021b). A three-dimensional parametric adult head model with representation of scalp shape variability under hair, Applied Ergonomics, 90: 103239

Reed, M.P. (2013). Development of Anthropometric Specifications for the Warrior Injury Assessment Manikin (WIAMan). Technical Report UMTRI-2013-38. University of Michigan Transportation Research Institute, Ann Arbor, MI

Reed, M.P. (2022). Development of Anthropometric Specifications for the Large-Male Warrior Injury Assessment Manikin (WIAMan). Technical Report UMTRI-2022-7. University of Michigan Transportation Research Institute, Ann Arbor, MI.

Reed, M.P. and Corner, B.D. (2013). Generation of a Midsize-Male Headform by Statistical Analysis of Shape Data. Technical Report UMTRI-2013-39. University of Michigan Transportation Research Institute, Ann Arbor, MI.

Reed, M.P., Ebert, S.M, and Corner, B.D. (2013). Statistical Analysis to Develop a Three-Dimensional Surface Model of a Midsize-Male Foot. Technical Report UMTRI-2013-40. University of Michigan Transportation Research Institute, Ann Arbor, MI.

Reed, M.P. and Ebert, S.M. (2013). The Seated Soldier Study: Posture and Body Shape in Vehicle Seats. Technical Report 2013-13. University of Michigan Transportation Research Institute, Ann Arbor, MI.

Reed, M.P., Manary, M.A., and Schneider, L.W. (1999). Methods for measuring and representing automobile occupant posture. Technical Paper 990959. Society of Automotive Engineers, Warrendale, PA.

Schneider, L.W., Robbins, D.H., Pflüg, M.A., and Snyder, R.G. (1983). Anthropometry of Motor Vehicle Occupants: Development of anthropometrically based design specifications for an advanced adult anthropomorphic dummy family, Volume 1. Final report DOT-HS-806-715. U.S. Department of Transportation, National Highway Traffic Safety Administration, Washington, DC.

Wang, Y., Cao, L., Bai, Z., Reed, M.P., Rupp, J.D., Hoff, C.N., and Hu, J. (2016) A parametric ribcage geometry model accounting for variations among the adult population. *Journal of Biomechanics*, 49(13): 2791-2798